ISIJ International, Vol. 43 (2003), No. 4, pp. 527–533

Hydrogen Trapping Behavior in Vanadium-added Steel

Hitoshi ASAHI, Daisuke HIRAKAMI and Shingo YAMASAKI

Steel Research Laboratories, Nippon Steel Corporation, Shintomi, Futtsu-city, Chiba 293-8511 Japan.

(*Received on August 29, 2002; accepted in final form on October 22, 2002*)

Hydrogen trapping and de-trapping behavior was investigated for steels with and without V. The de-trapping of hydrogen is very slow while the trapping presumably proceeds rapidly for steels containing VC precipitates. The activation energy for de-trapping is in the range of 33 to 35 kJ/mol. The trapped-hydrogen content and diffusible-hydrogen content in the steady state increase with increasing hydrogen entry rate into the steel. The density of hydrogen trapping sites decides the maximum trapped-hydrogen content; 9 ppm for 1 % V steel tempered at peak secondary hardening temperature. Analysis of hydrogen embrittlement cracking tests in terms of hydrogen contents such as the critical hydrogen content should be performed on the specimens with uniform hydrogen distribution and must consider the nature of hydrogen whether it is trapped or diffusible.

KEY WORDS: hydrogen embrittlement; hydrogen trapping; thermal desorption analysis; vanadium-added steel.

1. Introduction

Most hydrogen embrittlement, which prevents a steel from being used in extreme conditions, occurs as a result of the hydrogen that is generated on the surface through corrosion entering into the steel. The amount of hydrogen entering into the steel depends on the acidity of the environment in which the steel is exposed and the existence of a substance which accelerates the entry of hydrogen into the steel.[1] Furthermore, the rate of hydrogen entry often changes with time. The following examples are well known; (1) the change with time of hydrogen entry into a bolt exposed to an atmospheric environment due to wet and dry surface conditions and formation of corrosion products,[2] (2) the decay with time of hydrogen entry into steel exposed to a sour (wet hydrogen sulfide) environment due to sulfide formation on the surface.[3] Thus, steel products sometimes unexpectedly crack and sometimes do not. In order to understand these problems, it is necessary to know the change of hydrogen entry rate and the change of hydrogen content that contributes to hydrogen embrittlement. Regarding the latter, the use of hydrogen trapping is hoped to mitigate hydrogen embrittlement because hydrogen trapping decreases the amount of diffusible hydrogen that is thought to contribute to hydrogen embrittlement.

Under the conditions that hydrogen continuously enters into steel, it is thought that hydrogen trapping has no effect on hydrogen embrittlement because hydrogen enters into the steel even after the hydrogen trapping sites are occupied. On the other hand, in the case that hydrogen exists in the steel at the beginning and no other hydrogen enters into the steel such as in the case of cold cracking in welding, hydrogen embrittlement is thought to be mitigated because some of the hydrogen is trapped and thus the diffusible hydrogen content decreases. The hydrogen embrittlement cracking of high-strength bolts exposed to the atmosphere is estimated to be an intermediate condition between both cases. There, hydrogen enters into the bolts intermittently. Recently, it is reported that addition of vanadium (V) to the steel increases the resistance to hydrogen embrittlement of high-strength bolts[4] (this type of environmental cracking is generally called “delayed fracture” in Japan). An especially remarkable increase in delayed fracture resistance has been shown in atmospheric exposure tests.[4] This is probably because of hydrogen trapping in vanadium carbide (VC). The phenomena of hydrogen trapping in VC, however, are not well understood. Therefore, in order to further utilize V-added steel as steel resistant to environmental cracking, the features of hydrogen trapping in V-added steels were studied. The effects of hydrogen entry rate and hydrogen charging time were mainly investigated using V-added steels and V-free steels.

2. Experimental Procedure

2.1. Materials

Steels with varied V content were used in this study. The aiming contents of the chemical composition are listed in **Table 1**. To realize a fully martensitic microstructure, B was added. And steels were melted in a vacuum induction furnace, cast into 50 kg ingots, re-heated at 1 250°C and hot-rolled into 10 mm thick plates. The plates were

Table 1. Chemical compositions. (mass%)

	C	Si	Mn	P	S	V	Al	B	N
NA	0.25	0.3	1.5	0.008	0.0010	0	0.06	0.0010	0.0030
NB	0.25	0.3	1.5	0.008	0.0010	0.3	0.06	0.0010	0.0030
NC	0.25	0.3	1.5	0.008	0.0010	1.0	0.06	0.0010	0.0030

quenched and tempered under the conditions indicated in **Table 2**. Because prominent secondary hardening occurs in NC steel as shown in **Fig. 1**, two steels (NCF and NCG) having the same strength level and tempered at different tempering temperatures were prepared: one without clear precipitation hardening and the other with peak secondary precipitation hardening. The strengths of the steels are also shown in Table 2 and the microstructures were fully martensitic.

2.2. Hydrogen Charging Method

Hydrogen was electrically charged in an electrolyte of 3% NaCl solution with an addition of 3 g/*l* ammonium thiocyanate (NH_4NCS) at room temperature. The cathodic charge current was between 0.02 and 1.0 mA/cm^2. The hydrogen charging time was changed depending on the purpose.

2.3. Hydrogen Analysis

Thermal desorption analysis (TDA) of hydrogen was conducted using a gas chromatograph. The sampling time was in 5-min intervals and the heating rate was 100°C/h, unless otherwise indicated. A relatively thin specimen of 5 mm in diameter and 82 mm in length was employed in order to reduce the effect of hydrogen diffusion in the specimen.

Table 2. Heat-treatment conditions and tensile properties.

Steel	No.	Quench (WQ)	Temper (WC)	YS/MPa	TS/MPa
NA	NAA	930℃ − 30min.	600℃ − 30min.	631	765
	NAE	930℃ − 30min.	350℃ − 30min.	992	1117
NB	NBA	930℃ − 30min.	600℃ − 30min.	1031	1082
NC	NCF	1050℃ − 30min.	325℃ − 30min.	1319	1407
	NCG	1050℃ − 30min.	625℃ − 30min.	1193	1423

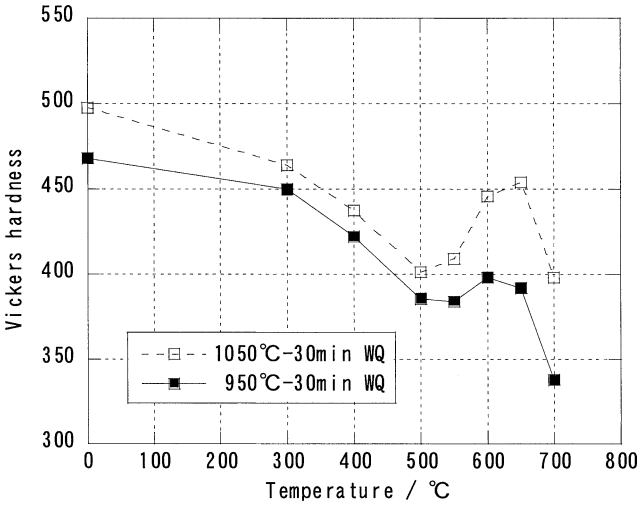

Fig. 1. Change in hardness with tempering temperature of NC steel.

2.4. Hydrogen Permeation Test

An electrochemical hydrogen permeation method with a nickel-plated specimen on the anode-side surface was used.[5] The cathodic hydrogen charging in the cathode-side chamber was conducted in the same way as indicated above. The specimen thickness was 1 mm. The steady state of the permeation rate, J was measured.

2.5. Hydrogen Embrittlement Cracking Test

The resistance to hydrogen embrittlement cracking was evaluated by a constant load test of the hydrogen-charged specimen. A notched tensile specimen with the dimensions indicated in **Fig. 2** was employed. Two tests different in hydrogen charging methods were conducted; a pre-charge method and a continuous-charge method. The applied tensile load was equivalent to 90% of the tensile strength at the cross section of the notch bottom. The maximum test time was 100 h.

(1) Pre-charge Method

The specimen was Cd-plated after electrically hydrogen charging in order to prevent the escape of hydrogen from the specimen. The hydrogen charging was performed for 6 h or 18 h. After the Cd-plating on the specimen surface to confine the hydrogen inside of the specimen, the specimen was kept at room temperature for 96 h to obtain uniform hydrogen distribution. The specimen was loaded and the failure time was measured. After the specimen failed or the test time terminated, the Cd-plating was removed and the hydrogen content in the specimen was measured by TDA.

(2) Continuous-charge Method

After the specimen was placed in the test cell and was loaded, hydrogen-charging started. After the specimen failed or the test time terminated, the specimen was removed from the test cell and the hydrogen content in the specimen was measured by TDA.

3. Results

3.1. Hydrogen Evolution Test Results

If the specimen is left at room temperature after being hydrogen-charged, so-called "diffusible hydrogen" is expected to diffuse out. **Figure 3** shows the results of hydrogen thermal evolution of the as-charged specimens and the specimens exposed at room temperature for NCF and NCG. In the cases of V-added steel tempered at a low temperature (NCF) and V-free steel (NAA) for which result is not indicated here, no hydrogen evolution was observed after a 24-h exposure, that is, all of the hydrogen had diffused out

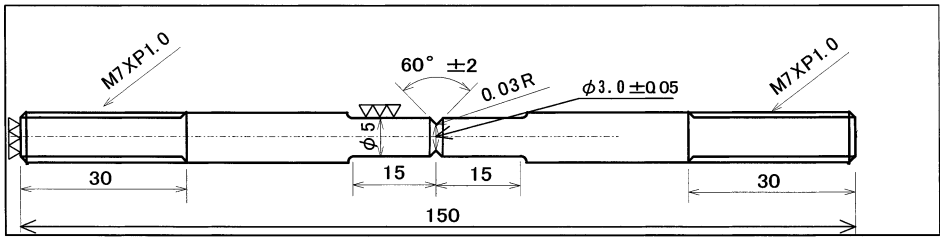

Fig. 2. Specimen of hydrogen embrittlement cracking test.

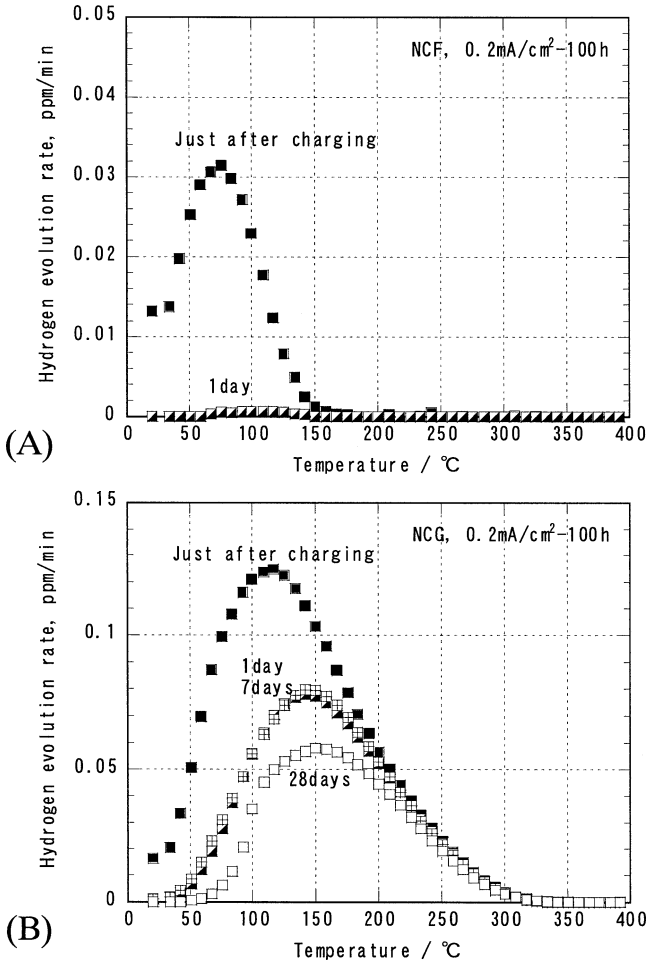

Fig. 3. Change in hydrogen evolution curve with exposure time at room temperature after hydrogen charging. (A) NCF, (B) NCG.

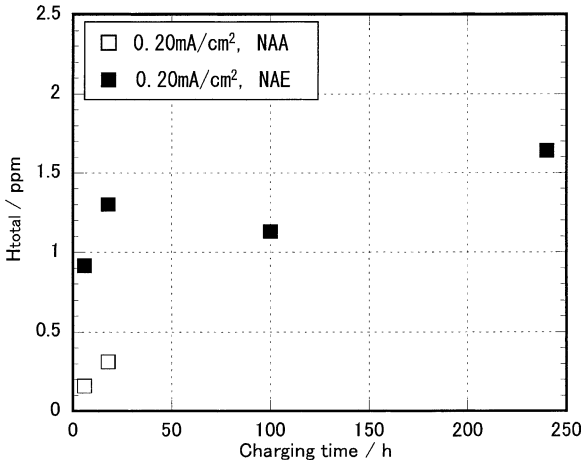

Fig. 5. Change in H_{total} with hydrogen charging time for NAA and NAE.

while the specimen was kept at room temperature for 24 h. On the other hand, a large amount of hydrogen remained in the specimen of V-added steel tempered at high temperatures at which V precipitates can be formed (NBA, NCG) after 24-h exposure. The remaining hydrogen was regarded as being trapped. These results clearly show that hydrogen trapping occurs in V-added steels tempered at temperatures at which V precipitates. In **Fig. 4**, decay curves of hydrogen

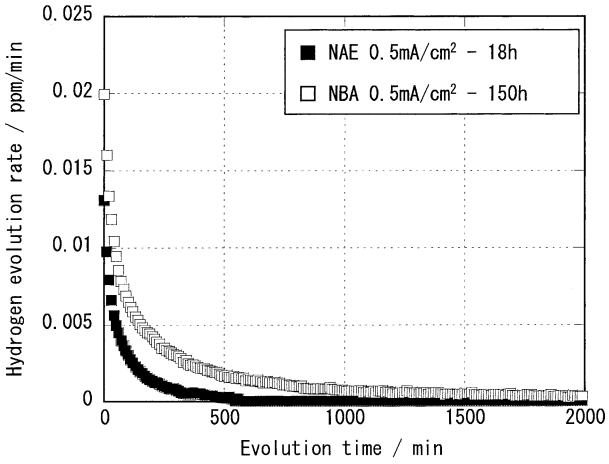

Fig. 4. Decay of hydrogen evolution rate at room temperature with time.

evolution at room temperature are illustrated for NAE and NBA. The hydrogen evolution sharply decreased with time within 24 h. Hence, in the present study, the following characterizing of hydrogen was employed: total hydrogen, H_{total}, the amount of hydrogen evolved at temperatures below 350°C by TDA, trapped hydrogen, H_{trap}, the amount of hydrogen remaining after 24-h exposure at room temperature, and diffusible hydrogen, $H_{dif}=H_{total}-H_{trap}$.

The change of hydrogen contents, H_{total} and H_{trap}, with time was measured for each steel. The results are illustrated with hydrogen charging time in **Figs. 5–7**. Figure 5 illustrates the results for steels NAA and NAE. H_{total} increased with charging time and saturated within 18 h for NAE and the same tendency is expected for NAA. The saturation of hydrogen content means that the steady state is achieved. No H_{trap} existed for these steels. As shown in Fig. 6 regarding NBA steel, H_{total} increased with charging time and saturated at around 100 h with all cathodic current densities but the increase rate of H_{trap} differed depending on current density although it is hard to describe the results accurately due to lack of some data. The time to the saturation is probably shortened with increasing current density. The results for NCG are illustrated in Fig. 7. H_{total} increased with charging time and became constant at about 100 h similar to NBA at a charge current of 0.05 mA/cm^2 or greater. It takes longer time for H_{total} to become the saturation value at the very small charge current of 0.02 mA/cm^2. H_{total} and H_{trap} at the steady state obtained from Figs. 6 and 7 are plotted in **Figs. 8** and **9** in terms of dependence on cathodic current density. In Fig. 8, the results for NBA are shown together with the hydrogen permeation current density at steady state. H_{total} increases with increasing current density and becomes constant at about 0.1 mA/cm^2. The permeation current density changes similarly. H_{trap} , however, is saturated at about 0.8 ppm at 0.05 mA/cm^2. In the case of NCG as shown in Fig. 9, both H_{total} and H_{trap} increased with increasing current density and became constant at about 0.1 mA/cm^2.

3.2. Determination of Activation Energy for Trapped Hydrogen

After the diffusible hydrogen diffused out during exposure at room temperature for 24 h, the activation energy, E_a, corresponding to the remaining hydrogen evolution peak

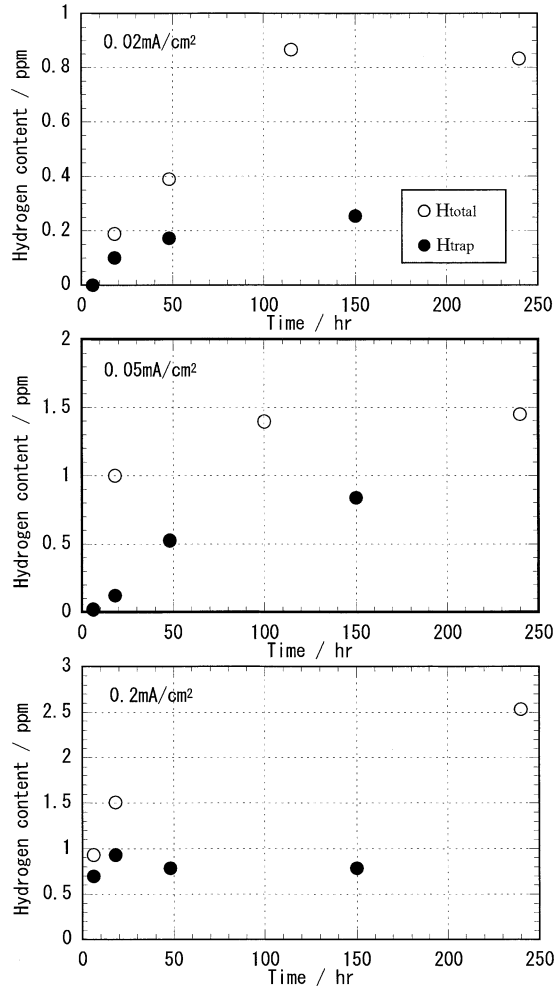

Fig. 6. Change in H_{total} and H_{trap} with hydrogen charging time for NBA.
(A) 0.02 mA/cm^2, (B) 0.05 mA/cm^2, (C) 0.20 mA/cm^2.

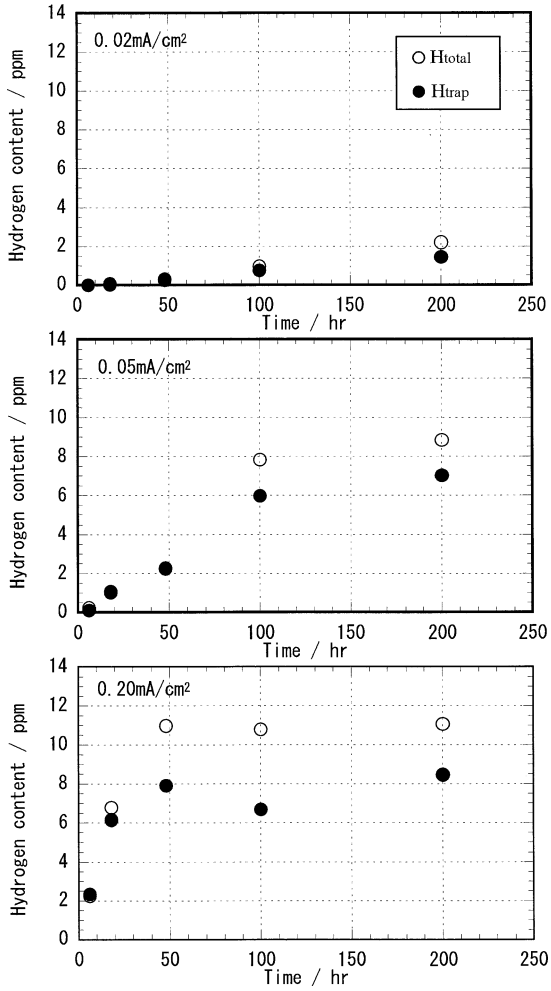

Fig. 7. Change in H_{total} and H_{trap} with hydrogen charging time for NCG.
(A) 0.02 mA/cm^2, (B) 0.05 mA/cm^2, (C) 0.20 mA/cm^2.

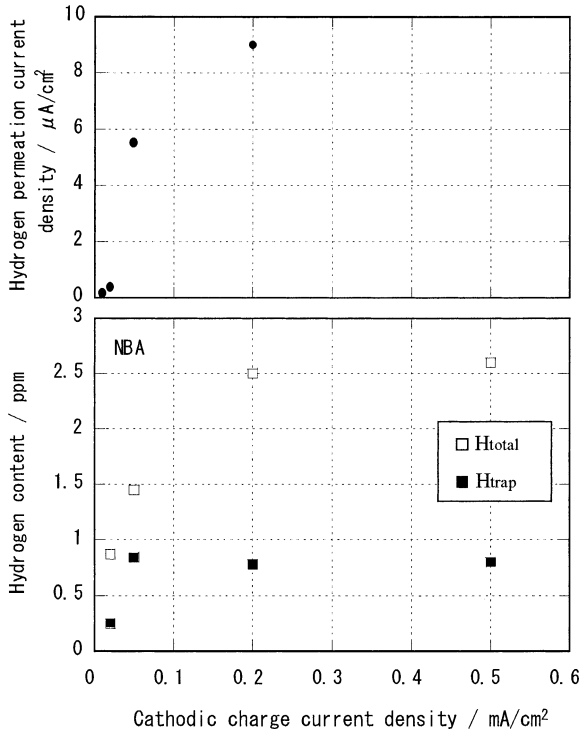

Fig. 8. Change in H_{total}, H_{trap} and permeation current at steady state with hydrogen charging current for NBA.

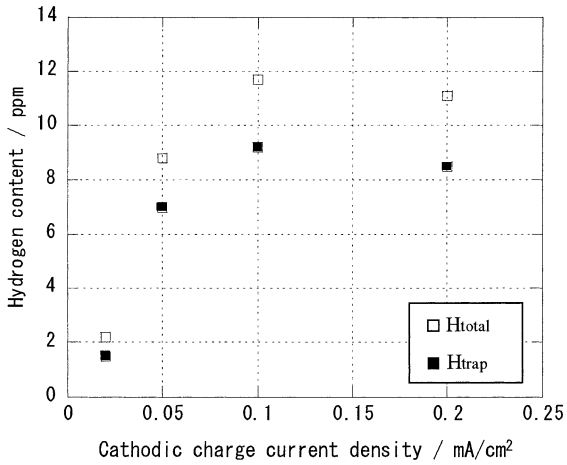

Fig. 9. Change in H_{total} and H_{trap} at steady state with hydrogen charging current for NCG.

was decided by the peak shift method using the following equation[6)]

$$E_a\phi/RT_c^2 = A\exp(-E_a/RT_c)$$

where ϕ=heating rate, A=constant, R=gas constant, T_c=peak temperature.

The specimen was hydrogen-charged at an electric cur-

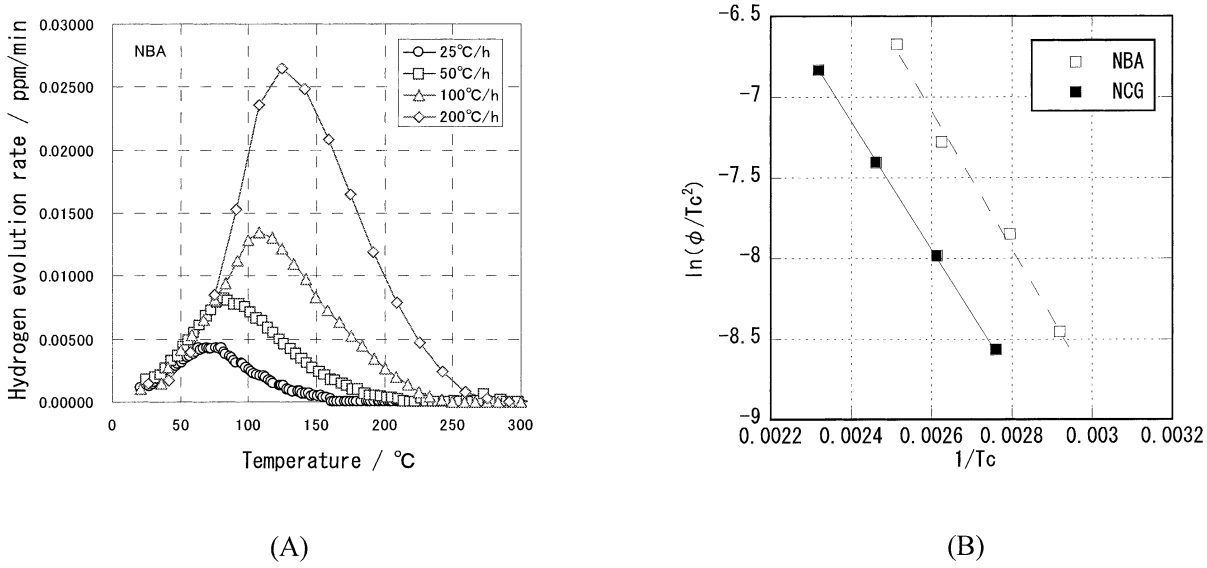

Fig. 10. Determination of activation energy for de-trapping. (A) Change in hydrogen evolution curve with heating rate for NBA. (B) substitution of peak temperature and heating rate for the equation used for the peak shift method.

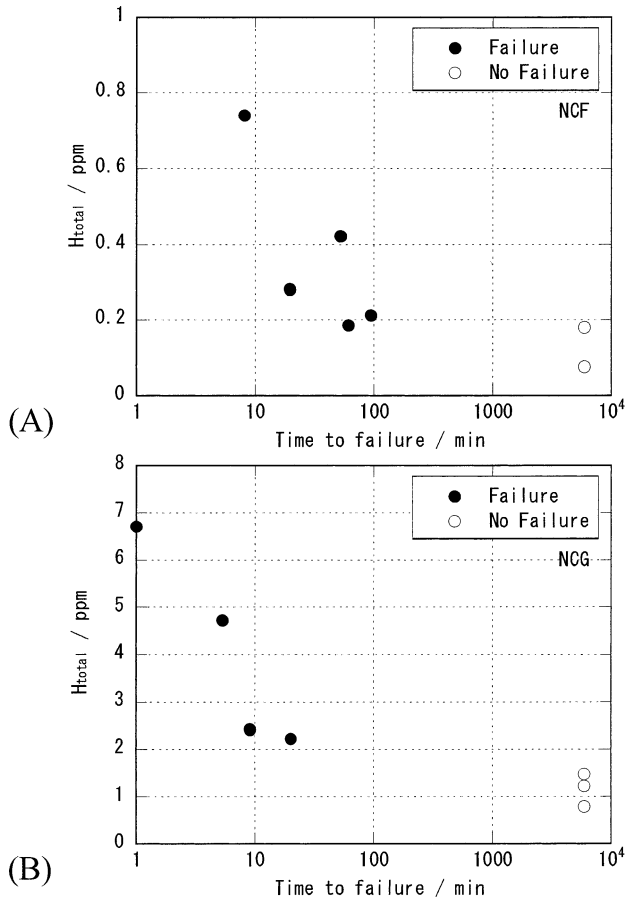

Fig. 11. Hydrogen embrittlement cracking test results for the pre-charge tests on (A) NCF and (B) NCG.

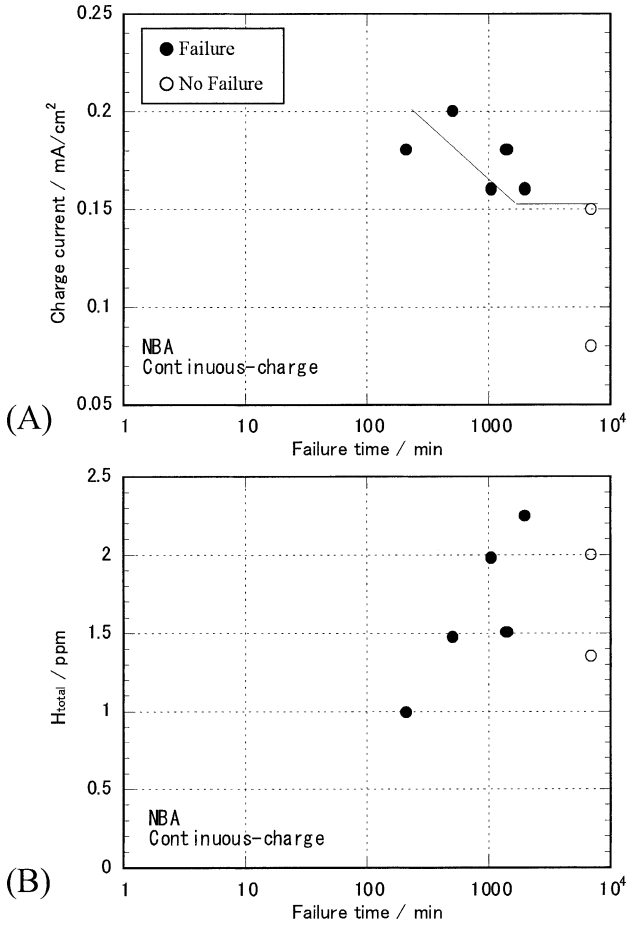

Fig. 12. Hydrogen embrittlement cracking test results for the continuous-charge test on NBA.

rent density of 0.2 mA/cm^2 for 100 h, where the steady state is achieved. The change of hydrogen evolution curves is indicated for NBA in **Fig. 10**(A), for example. The hydrogen evolution rate is smaller for a lower heating rate because the sampling interval is constant but the total evolved hydrogen amount is constant. The results of the peak shift analysis are illustrated in Fig. 10(B). The activation energies thus obtained were 35.3 kJ/mol and 32.6 kJ/mol intended for NBA and NCG, respectively.

3.3. Hydrogen Embrittlement Cracking Test Results

Hydrogen embrittlement cracking test results are shown in **Figs. 11** and **12**. For the pre-charge tests on NCF and NCG, the relations between H_{total} and failure time are illustrated in Figs. 11(A) and 11(B). The time to failure in-

creased with decreasing H_{total}. The critical hydrogen content, H_{crt}, that is the maximum H_{total} at which no failure occurs is estimated to be 0.18 ppm for NCF and 1.5 ppm for NCG. In Fig. 12(A), the continuous-charge test results of NBA are illustrated in the relation between charge current density and failure time. The same test results are re-plotted in terms of H_{total} instead of current density in Fig. 12(B). No failure occurred at a current density of 0.15 mA/cm^2 or lower. The H_{total} corresponding to 0.15 mA/cm^2 is 2 ppm.

4. Discussions

4.1. Nature of Hydrogen Trapping

The behavior of trapping and de-trapping of hydrogen was investigated for steels with and without V. A large amount of hydrogen trapping occurs in V-added steels. The trapping site is estimated to be VC for the following reasons. First, the trapping sites are thought to be vanadium precipitates because no hydrogen trapping was observed for V-free steel (NA) and low-temperature tempered V-added steel (NCF), and the amount of trapped hydrogen increased with an increase in V addition. It is reasonable that the V precipitate is determined to be VC because most of N is fixed as AlN and thus VN cannot be formed although no direct observation on precipitates was performed in the present study.

The activation energies for de-trapping of hydrogen for NBA and NCG were determined to be 35.3 kJ/mol and 32.6 kJ/mol, respectively. Both values are thought to be equal considering experimental error. Yamasaki *et al.* reported that the activation energy for VC in 0.35 V mass% steel is 36 kJ/mol,[4] which is very close to the values in this study. This fact suggests that the characteristic of VC as a trapping site does not change regardless of V content and tempering condition. The difference between NBA and NCG is probably only the difference in density of VC and hydrogen trapping amount per VC. When the activation energy was determined for NCG that was charged at 0.1 mA/cm^2 for 18 h and kept at room temperature for 24 h, the value was decided to be 44 kJ/mol.[7] This value is probably wrong because the distribution of hydrogen in the specimen was estimated to be not uniform; hydrogen concentration was higher near the surface. This suggests that the specimen with strictly uniform hydrogen distribution must be used.

So far, the activation energies have been reported for various trapping sites. The activation energy for TiC is reported to be 86.9 kJ/mol,[8] much larger than for VC. The activation energy for VC is larger than that for grain boundary of 17.2 kJ/mol[9] and that for dislocation of 26.8 kJ/mol[9] or 27 kJ/mol[10] and is equivalent to that for microvoid of 35.3 kJ/mol.[9]

The change of H_{total} and H_{dif} occurs rather synchronously while the decay of H_{trap} is very slow. This suggests that diffusible hydrogen is quickly trapped at a trap site. In the case of NBA, the maximum H_{trap} is 0.8 ppm and the saturated H_{dif} is 1.8 ppm. Because the H_{trap} of 0.8 ppm remains constant when H_{total} increases, it is judged that all the trap sites are filled in this state. Thus, the maximum H_{trap} represents the hydrogen trap density. In the case of NCG, the maximum H_{trap} is 9 ppm and the saturated H_{dif} is 3 ppm, where H_{total} is 12 ppm. The high value of H_{trap} indicates that the hydrogen trapping sites are present in a high density probably because of the high V content of 1.0 % and the tempering at temperature corresponding to a peak of secondary hardening.

4.2. Meaning of the Critical Hydrogen Content

The steels NCF and NCG have almost the same tensile strength but different critical hydrogen contents, H_{crt}; 0.18 ppm for NCF and 1.5 ppm for NCG. This does not necessarily mean that NCG is more resistant to hydrogen embrittlement cracking than NCF. In the following, the constituents of hydrogen in the steels will be discussed. The amount of H_{dif} among the H_{crt} can be estimated to be 0.18 ppm for NCF and 0.38 ppm [1.5 ppm×(3 ppm/12 ppm)=0.38 ppm] for NCG if the ratio of H_{dif} to H_{total} mentioned above is assumed. Then, the change of H_{dif} with the cathodic current density is examined. At the current density of 0.2 mA/cm^2, the saturated values of H_{dif} are 1.4 ppm for NCF and 3 ppm for NCG; H_{dif} of NCG is about two times larger than that of NCF for a constant hydrogen entry rate; 0.18 ppm for NCF and 0.38 ppm for NCG is achieved for the same current density. Thus, both NCF and NCG crack at about the same hydrogen entry rate, that is, in the same environment if the hydrogen entry is continuous. This indicates that the contribution of the hydrogen trapping by VC to the increase in resistance to "delayed fracture" is expected only for the intermittent hydrogen entry into the steel.

The H_{crt} of NBA was 2 ppm and H_{dif} among H_{crt} can be estimated to be 1.2 ppm [=2−0.8]. At shorter times, however, failure occurred at H_{total} lower than 2 ppm as shown in Fig. 12(B). This is probably because the hydrogen content near the surface is higher than that inside. Figure 6 shows that it takes about 100 h to reach the steady state. The use of average hydrogen content before reaching the steady state may mislead the discussion. This point should be noted.

5. Conclusions

The behavior of trapping and de-trapping of hydrogen was investigated for steels with and without V. The important results obtained are as follows.

(1) Hydrogen trap sites of V-added steel with tempered martensite structure are estimated to be vanadium carbide. The activation energy for de-trapping is in the range of 33 to 35 kJ/mol. The de-trapping of hydrogen is very slow while the trapping presumably proceeds rapidly.

(2) Trapped-hydrogen content and diffusible-hydrogen content increase with hydrogen charging time and become steady state at about 100 h for the specimen of 5 mm in diameter.

(3) Trapped-hydrogen content and diffusible-hydrogen content in the steady state increase with increasing hydrogen entry rate into the steel. The density of hydrogen trapping sites decides the maximum trapped-hydrogen content. For 1 % V steel tempered at peak secondary hardening temperature, the maximum trapped-hydrogen content is 9 ppm.

(4) Analysis of hydrogen embrittlement cracking tests in terms of hydrogen contents such as the critical hydrogen

content should be performed on the specimens with uniform hydrogen distribution and must consider the nature of hydrogen whether it is trapped or diffusible.

Acknowledgements

This work was sponsored by the Ministry of Education, Culture, Sports, Science and Technology.

REFERENCES

1) H. Asahi, M. Ueno and T. Yonezawa: *Corrosion*, **50** (1994), 537.
2) K. Yamakawa: Advances in Delayed Fracture Solution, ISIJ, Tokyo, (1997), 77.
3) M. Kimura: Corrosion and Corrosion Resistant Materials in The Oil & Gas Industry ed. by K. Yamakawa, Japan National Oil Corporation, Tokyo, (1998), 111.
4) S. Yamasaki and T. Takahashi: *Tetsu-to-Hagané*, **83** (1997), 454.
5) S. Yoshizawa, T. Tsuruta and K. Yamakawa: *Corros. Eng.* (*Jpn*), **24** (1975), 511.
6) W. Y. Choo and J. Y. Lee: *J. Mater. Sci.,* **17** (1982), 1930.
7) H. Asahi and T. Hirakami: Roles of Hydrogen in Environmental Embrittlement of Structual Steel, ISIJ, Tokyo, (2002), 75.
8) H. G. Lee and J. Y. Lee: *Acta Metall.,* **32** (1984), 131.
9) W. Y. Choo and J. Y. Lee: *Metall. Trans. A,* **13A** (1982), 135.
10) H. Hagi and Y. Hayashi: *J. Jpn. Inst. Met.*, **51** (1987), 24.